DNA Replication, Chromatin Structure, and Histone Phosphorylation Altered by Theophylline in Synchronized HeLa S3 cells

THOMAS W. DOLBY, ANDREW BELMONT, THADDEUS W. BORUN, and CLAUDIO NICOLINI

The Wistar Institute of Anatomy and Biology, Philadelphia, Pennsylvania 19104, and Department of Physiology-Biophysics, Temple University, Philadelphia, Pennsylvania 19122

ABSTRACT The onset of DNA replication normally is coincident with an increase in histone 1 phosphorylation and a relaxation in chromatin structure. In this paper we show that 5 mM theophylline, added 2 h after selective detachment to synchronized HeLa-S-3 cells, delays the onset and reduces the rate of DNA synthesis while theophylline treatment beginning at 8 h has no effect on subsequent DNA synthesis. These actions of theophylline are accompanied by an inhibition of histone 1 phosphorylation and a prevention of the normal relaxation in chromatin structure between G1 and S phases as revealed by image analysis of Feulgen-stained nuclei. The time courses of intracellular cyclic AMP levels, nonhistone protein phosphorylation, and [^{3}H]lysine incorporation are also compared in the same treated and untreated synchronized HeLa cells. Comparison with experiments using 1-β-D-arabinofuranosylcytosine (Ara-C) shows that the above phenomena are not a direct result of inhibition of DNA synthesis. We interpret our results as evidence that the associations between histone 1 phosphorylation, chromatin relaxation, and the onset of DNA synthesis are temporally and causally related.

Variations in chromatin structure during the cell cycle have been well documented using a variety of biochemical and biophysical probes. In the past several years these studies have been extended to chromatin in the intact cell using techniques such as flow microfluorimetry or image analysis of Feulgen-stained nuclei. This capability not only has the potential of circumventing certain of the artifacts introduced by isolation by bulk chromatin but also allows observations of the properties of chromatin from individual cells. Interestingly, it was found that changes in nuclear-DNA morphology during the HeLa cell cycle (1), as well as in diploid fibroblasts after stimulation (2) or virus transformation (3), correlate well with alterations in isolated chromatin structure and its functional state as measured by template activity, circular dichroism, and the number of primary binding sites of intercalating dyes (4). Specifically, increases in average optical density (AOD) or form factor (FF) (area/[perimeter]^2) or nuclear-stained DNA *in situ* were associated with decreases in template activity, circular dichroism at 272 nm, and the number of primary dye binding sites all measured in vitro.

Moreover, image analysis of single cell nuclear chromatin revealed that the modulation of structure during the HeLa cell cycle was much more pronounced than suggested by the average properties of isolated chromatin from synchronized populations. In particular, image analysis of individual cells coupled with autoradiography indicated that what had appeared as a gradual and continuous transition from a maximally condensed chromatin at 5 h after mitosis ("middle G_1") to a maximally relaxed chromatin at 12 h after mitosis ("middle-S") (5, 6) was actually most likely a more abrupt transition from a maximally condensed late G_1 nucleus with high AOD and high FF to a maximally relaxed early S nucleus with low average optical density and low form factor (7). Exposure of synchronized cells to 1-β-D-arabinofuranosylcytosine (Ara-C), a drug that blocks DNA synthesis by the inhibition of DNA polymerase and ligase enzymes, resulted in cells containing 2c DNA content arrested at the G_1-S border in the relaxed conformation of early S nuclei, thus proving that the transition from a condensed to relaxed morphology was not a result of DNA synthesis but perhaps a prerequisite (8).

Biochemical studies have associated an increase in one type of histone 1 phosphorylation with the onset of DNA synthesis (9–18). (Another type of histone 1 phosphorylation, presumably occurring at different sites, has been linked by Rattle et

THE JOURNAL OF CELL BIOLOGY · VOLUME 89 APRIL 1981 78-85

al. [19] to condensation of chromatin from G_2 to mitosis. However, as shown experimentally [20], and indicated on general theoretical grounds,[1] the influence of phosphorylation on histone 1-DNA interactions is strongly site-specific.) Later circular dichroism measurements coupled with thermal denaturation studies indicated that changes in the interactions of histone 1, DNA, and nonhistone chromosomal proteins were associated with the phosphorylation of H1 and appeared to be responsible for the relaxation of the compact G_1 chromatin into a more open or relaxed S-phase configuration (5).

This last conclusion was of great interest in light of the known influence of cyclic nucleotide levels on the phosphorylation state of various proteins and the more recent associations between changing cyclic nucleotide levels and cell proliferation. Specifically, increases in cyclic AMP levels have been observed in many (21–25), but not all (26, 27), types of cells as they approach quiescence, while increased intracellular levels in cyclic AMP levels produced either by exogenous dibutyryl cyclic AMP (28–31), dibutyryl cyclic AMP in conjunction with phosphodiesterase inhibitors (29–32), or phosphodiesterase inhibitors alone (33–35), inhibit cell proliferation. Indeed, the action of certain phosphodiesterase inhibitors, including theophylline and caffeine, has been shown to involve a shift of untransformed cells from G_1 to G_0 (33, 35) as well as a cell cycle arrest in G_2 (33). Most interestingly, it was found that caffeine reduces mitotic delay of cells exposed to ionizing radiation (35). Both elevated concentrations of Ca^{++} and Mg^{++} salts, as well as hormone treatment, have also been shown to reduce mitotic delay after irradiation, and in both cases this has been linked to the state of chromatin condensation (35). Thus, in an attempt to determine whether there actually existed a causal relationship between histone 1 phosphorylation and chromatin structure, we were prompted by the above associations to explore the effect of theophylline on progression of synchronized HeLa cells from mitosis to S phase with attention focused on possible alterations in the normal modulation of chromatin structure during G_1 and S phases and associated changes in histone 1 phosphorylation while also monitoring cyclic AMP levels and nonhistone chromosomal protein phosphorylation (NHCP).

MATERIALS AND METHODS

Materials

Joklik-modified Eagle's minimal essential medium (medium A), Earle's balanced spinner salt solution, calf serum, and fetal calf serum were purchased from Grand Island Biological Co. (Grand Island, N. Y.). Thymidine, cytosine arabinoside-HCl, cycloheximide, thophylline, and amino acids were purchased from Sigma Chemical Co. (St. Louis, Mo.). Carrier-free [^{32}P]orthophosphoric acid, [2-^{14}C]thymidine, and [^{3}H]lysine were obtained from New England Nuclear (Boston, Mass.).

Methods

CELL CULTURE AND SYNCHRONIZATION: Logarithmically growing HeLa S-3 cells were maintained in suspension culture at 37°C at concentrations of between 2×10^5 and 5×10^5 cells/ml in Joklik-modified Eagle's minimal essential spinner medium supplemented with 3.5% each (vol/vol) fetal calf and calf serum.

The basic procedure for selective detachment of mitotic cells on a small scale has been published by Terasima and Tolmach (36) and Robbins and Marcus (37). The labeling index (LI) and mitotic rate (MR) were determined by autoradiography (6), on aliquots of cells at various time intervals after selective detachment: at $t = 0$ h, ~90% of the cells are in mitosis; at $t = 3.0$ h with LI = 5% and MR = 3%, ~90% of the cells are in "G_1 phase"; at $t = 11$ h, the cells are at the peak of DNA synthesis with LI = 83% and MR = 1% ("S phase"). At later times after mitosis, the degree of synchrony is markedly reduced (6), even though a large number of cells are in the G_2 phase between 14 and 18 h. Large quantities of selectively detached synchronized HeLa S-3 cells were prepared as described (38).

In each experiment the total yield of M-phase cells was about $3–4 \times 10^5$ cells/ml in a final volume of 1,800 ml. 90–95% of the cells were found to be in mitosis by phase-contrast microscopy. The cells were maintained in suspension culture and harvested as indicated below.

^{32}P LABELING: To estimate the rate of ^{32}P incorporation into histone 1 components, we removed synchronized cells at various times after mitosis, harvested them by centrifugation, and incubated them in phosphate-free medium A, supplemented with 2% fetal calf serum and ^{32}P at concentrations indicated in the figure legends. Inhibitors were present during labeling at the concentrations used for pretreatment.

CELL FRACTIONATION AND HISTONE EXTRACTION: Cells were harvested by centrifugation and fractionated at 3°C. Cell pellets were washed with Earle's spinner salt solution, 80 mM NaCl, 20 mM EDTA, 1% Triton X-100, and 0.15 M NaCl, as previously described (9, 39). Histones were isolated by extracting the resultant nuclear pellets three times with 0.6 ml of 0.25 N H_2SO_4. Pooled extracts were then dialyzed against 0.9 N acetic acid.

ELECTROPHORESIS: After dialysis, histones were resolved according to the method of Balhorn et al. (14) using 25 cm, 15% polyacrylamide gels containing 2 M urea and 0.9 N acetic acid. For total histone mass estimations, gels were run at 190 V for 22 h at room temperature. Total histone mass was determined by calculating the area under curves corresponding to the five main histone fractions obtained by scanning stained gels at 630 nm in a Gilford spectrophotometer (Gilford Instrument Laboratories Inc., (Oberlin, Ohio) (12). To separate phosphorylated histone 1 components, we ran duplicate gels at 200 V for 68 h at 4°C. Gels were stained with fast green and destained electrically as previously described (9). To determine ^{32}P radioactivity in histone 1 components, we sliced stained gels and digested them in H_2O_2 and counted as previously described.

CYCLIC AMP DETERMINATION: At the times indicated in the figure legends, 100 ml (4×10^7 cells) of synchronized cells were harvested at 37°C at 600 *g*. Cell pellets were washed in cold spinner salts, repelleted, and extracted three times, 10 vol (1 ml) 0.36 N perchloric acid containing a total of 430 cpm [^{3}H]-cyclic AMP to account for sample recovery. Extensive control studies show that this tracer cyclic AMP does not interfere with endogenous cellular determinations. The extracted supernates were pooled and neutralized with 1 N KOH and centrifuged at 1,000 *g* to remove K perchlorate. The supernates were applied to 4×0.7 cm columns of AG1X2 resin, washed with distilled H_2O followed by 2 M formic acid to elute cyclic AMP. Cyclic AMP was lyophilized, and aliquots were assayed in triplicate using the competitive binding protein assay provided by Amersham Corp. (Arlington Heights, Ill.). The assay was calibrated to a range of 0.14–16 pmol. The data are expressed as picomoles cyclic AMP/10^6 cells after recovery corrections and are a result of three independent experiments.

STAINING: Smears were prepared from the same synchronized cultures, either treated or untreated, at 3, 5, 8, 12, 15, and 18 h after selective detachment. All smears were hydrolyzed with 1 N HCl for 15 min and stained in parallel with Schiff reagent for 1 h according to the method of DeCosse and Aiello (40). After staining, the samples were mounted in Canada balsam.

IMAGE ANALYSIS: Nuclear images were magnified by a Zeiss Ultraphot microscope equipped with a × 100 oil immersion planar achromat of 1.25 NA. Illumination was provided by a condenser of 1.3 NA and a 100-W tungsten halogen light source equipped with a 540-nm filter with a half-band width of 40 nm. The image was registered on a plumbicon scanner by means of a Reichert high quality magnification changer. Total magnification was 1250. The image analyzer was the Quantimet Image Analyzing Computer (Cambridge Instrument, Co., Inc., Ossining, N. Y.) equipped with a 720-D densitometer. The scanner area is divided into 880 × 588 picture elements whose optical density can be digitized into 64 grey levels. By means of a stage micrometer (American Optical Corp., Scientific Instrument Div., Buffalo, N. Y.) the dimensions of each picture element was determined as $(0.08 \times 0.08)\ \mu m^2$. A blank area of each slide was used to load the shade corrector and to calibrate the densitometer by means of neutral density filters. A threshold of 0.06 OD was used to define the nuclear border. Field uniformity measurements on a single nucleus using nine positions around the field yielded for all slides, coefficients of variation of <2.5% for integrated optical density and 1.0% for area. Variation of both parameters was <0.5% for 10 consecutive measurements of a single image in the center of the field.

A number of basic parameters were measured for each nuclear image, and from these basic parameters several additional derived parameters were computed. Basic parameters included integrated optical density (IOD, proportional to DNA amount), area, perimeter, horizontal and vertical Feret diameters, and

[1] Belmont, A., and C. Nicolini. Polyelectrolyte theory and chromatin-DNA quaternary structure: Role of ionic strength and H1 histone. *J. Theor. Biol.* Manuscript submitted for publication.

horizontal and vertical complex projections. The horizontal and vertical Feret diameters (FD) are defined as the shadow projections of the image onto horizontal and vertical lines, respectively. The vertical and horizontal complex projections (CP) are defined instead as the sums of the shadow projections of all lagging edges on horizontal and vertical lines, respectively.

As a means of estimating border reentrance, an excess projection (EP) was defined as the numerical difference between a CP and its corresponding FD. Thus, EP_1 = CP (horizontal) − FD (vertical) and EP_2 = CP (vertical) − FD (horizontal). To reduce the influence of an image's orientation with respect to the direction of scanning, euclidean norms of EP and CP were then used to calculate a derived parameter, the convolution factor, defined as the euclidean norm of the excess projection, EP, divided by the euclidean norm of the complex projection, CP. Additional derived parameters calculated, which are essentially independent of orientation, were the AOD (IOD/area) and a normalized FF ($4\sqrt{}$ [area]/[perimeter]^2). The convolution factor, again a measure of border reentrance, was useful in interpreting the geometric significance of the form factor (which is only an index of the circularity and which is less than unity either for features which are completely nonreentrant but noncircular or approximately circular but which are also reentrant).

RESULTS

In confirmation of earlier reports, exposure of synchronized HeLa cells to a 5-mM concentration of theophylline beginning 2 h after selective mitoic detachment produced a partial arrest of cells in G_1. As shown in Fig. 1, [^{14}C]thymidine incorporation for the theophylline-treated cells remains at baseline values until ~12 h after mitosis at which time detectable DNA synthesis begins to occur. In comparison, in the control population, [^{14}C]thymidine incorporation rises sharply beginning at ~5 h after mitosis, reaching a peak at slightly after 10 h.

Examination of the image analysis data further clarifies the situation. It is apparent from the IOD vs. cell number histograms, seen in Fig. 2 as the projection along the *x* axis of the respective two-parameter histograms, that the slow rise in thymidine incorporation occurring at 12 h in the theophylline-treated population (Fig. 2*B*, panel *d*) is caused by a small fraction (15%) of the cells progressing through early S phase, while the majority of the cells are blocked with 2c DNA content. The fraction of cells which manages to pass the block and progress through S slowly increases with time, reaching roughly 50% at 18 h (Fig. 2*B*, panel *f*). Moreover, a rough estimate of S-phase duration, produced by focusing on the number of cells in early S (2.1C-3C) and late S and G_2 (3C-4C) vs. time, reveals that those cells that escape the G_1 (or G_1-S border) block progress through S phase at a slower rate than normal. Indeed, whereas at 8 h in the control slide there are only 61/200 cells in early S (the majority with DNA content in the range 2.1-2.5C), at 12 h there are 96/200 in late S and G_2. Yet, for the theophylline-treated cells, while at 12 h there are 30/200 cells in early S, at 15 h there are only 16/200 cells in late S and G_2. Similarly, while at 15 h there are 57/200 cells in early S and 16/200 cells in late S and G_2, at 18 h there are only 21/200 cells in late S and G_2.

This action of theophylline cannot be attributed simply to a direct inhibition of the cellular apparatus for DNA synthesis or to a generalized toxic effect. Returning to Fig. 1, we see that administration of the same theophylline concentration at 8 h after mitosis produces no change in [^{14}C]thymidine incorporation relative to the control. Experiments examining the uptake of media [^{14}C]thymidine in the presence or absence of theophylline show no significant alteration of intracellular transport within a 1-h treatment up to at least 10 h postmitosis (data not shown). In addition, not only have other investigators demonstrated the reversibility of theophylline's action (33), but also [^{3}H]lysine incorporation was found to be identical for the control and theophylline-treated cells between 3 and 10 h after

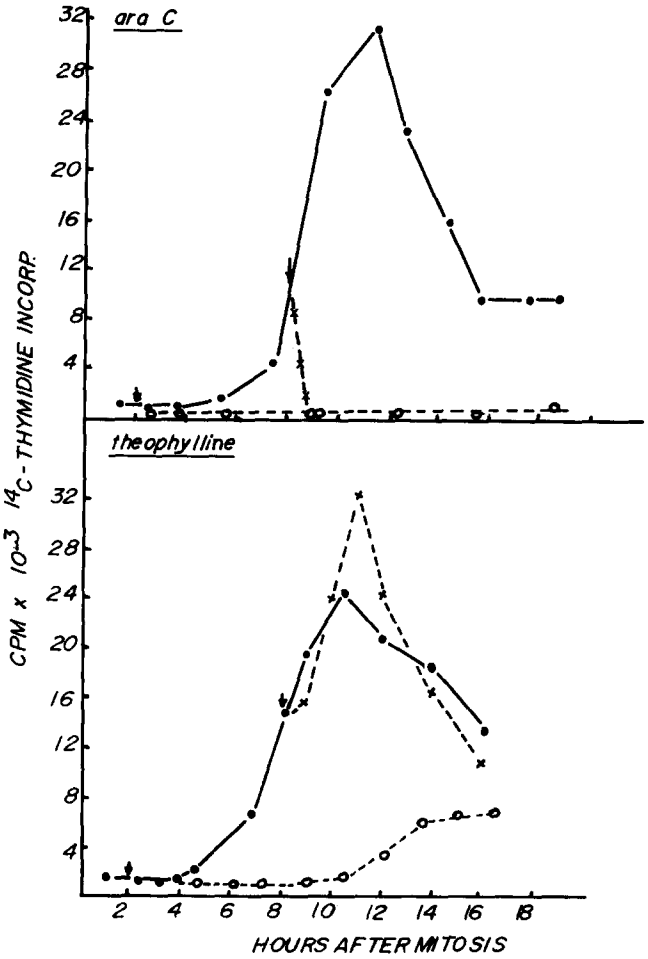

FIGURE 1 The effects of Ara-C and theophylline on [2-^{14}C]thymidine incorporation during the HeLa S-3 cell cycle. *Upper panel:* HeLa S-3 cells were collected in mitosis, resuspended in 300 ml of medium A at 3 × 10^5 cells/ml and incubated at 37°C for 18 h. 100 ml of the culture was removed at 2 h after mitosis (G_1) and treated with 40 μg/ml Ara-C. 100 ml was removed at 8 h after mitosis (S) and similarly treated. 2-ml samples were removed from the control and Ara-C-treated cultures at the indicated times, pulse-labeled with 0.2 μCi [2-^{14}]thymidine for 30 min at 37°C, and the radioactivity incorporated in 5% TCA-precipitable material was determined as previously described (5). ●, Control; ×, Ara-C added at 8 h; ○, Ara-C added at 2 h. *Lower panel:* A similar experiment using 5 mM theophylline instead of Ara-C. ●, Control, ○, theophylline added at 2 h; ×, theophylline added at 8 h.

mitosis (data not shown). Thus, theophylline does not appear to be affecting the overall protein synthesis rate (in particular, the synthesis of lysine-rich histone would seem to be unaffected).

As anticipated, however, the action of theophylline is associated with a dramatic change in the pattern of histone 1 phosphorylation as shown in Fig. 3. After pulse-labeling control and drug-treated cells with ^{32}P at 2 and 9.5 h after mitosis as described in the legend to Fig. 3, histone was extracted as described in Materials, and histone 1 components were resolved by extended electrophoresis on long polyacrylamide gels (14). It may be seen in the upper left panel of Fig. 3 that histone 1 components extracted from control G_1 cells migrate in these gels as two principal peaks (forms I and II) which incorporate rather low amounts of ^{32}P during the 75-min labeling period. As control cells enter S phase, the apparent rate of ^{32}P incor-

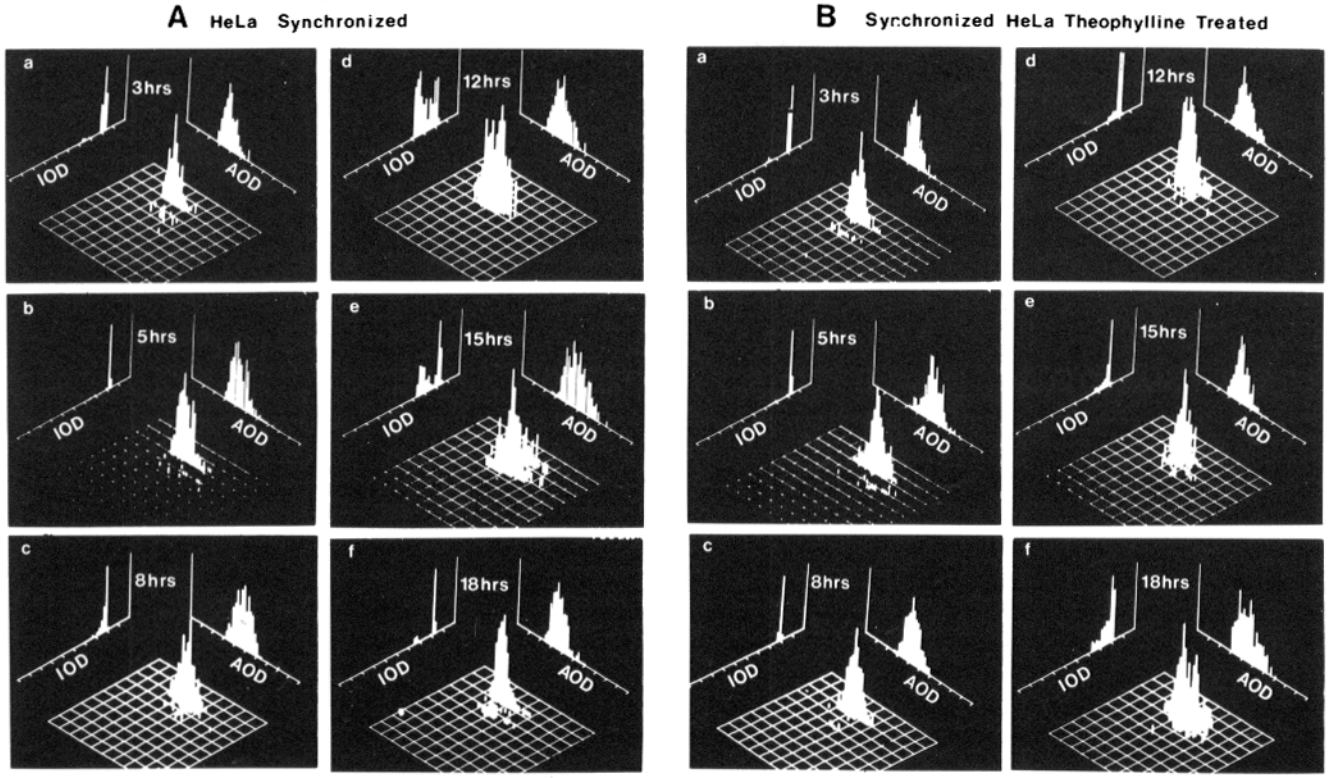

FIGURE 2 (*A*) Time sequences of the IOD vs. AOD histograms for the control populations. The Z axis corresponds to cell number. In all cases, the range of IOD is 0–10,000 and the range of AOD, 0–100. Histograms *a*, *b*, *c*, *d*, *e*, and *f*, correspond to 3, 5, 8, 12, 15, and 18 h, respectively, after selective detachment. The total sample population at each time point was 200 cells. (*B*) Same as above, but in this case the data displayed correspond to the theophylline-treated cells.

poration into histone 1 increases 10-fold (9) and the migration of phosphorylated histone 1 components is retarded such that three principal peaks (forms II and III) are now resolved by gel electrophoresis (upper right panel, Fig. 3). Recent experiments (41) indicate that the three peaks of histone 1 in HeLa cells resolved under these conditions represent complex mixtures of two distinct molecular components: (*a*) mol wt ~20,000; (*b*) mol wt ~21,000. During S phase, these components acquire more phosphate groups that retard their migration. However, 5-mM theophylline treatment from 2 to 10.75 h after mitosis significantly inhibits the apparent level of histone 1 ^{32}P incorporation and causes histone 1 components to remain as rapidly migrating protein species that are smaller than those normally found in G_1 cells. In contrast, Ara-C treatment beginning 2 h after mitosis at a concentration (40 μg/ml) completely inhibits subsequent DNA synthesis but not phosphorylation of previously synthesized histone 1 components (9) which also migrated as the three principal peaks, as again seen in Fig. 3, even though the apparent level of histone 1 phosphorylation was cut in half. This implies that the influence of theophylline on histone 1 phosphorylation is not simply a result of the inhibition of DNA synthesis. While histone 1 phosphorylation is reduced in theophylline-treated cells, nonhistone phosphorylation at 10 h after mitosis is increased relative to control cells with marked increases in certain protein species (data not shown). Thus, it appears that theophylline can potentiate some NHCP phosphorylations while greatly inhibiting histone H1 phosphorylation and the progression of DNA synthesis.

In light of previous suggestions discussed in the introduction, correlating the onset of DNA synthesis with the relaxation of chromatin in cells at the G_1-S boundary and correlating this change in chromatin conformation with increases in histone 1 phosphorylation, attention must now be devoted to an examination of the variations in nuclear morphology induced by theophylline treatment. This may be accomplished by studying Table I, which summarizes the average values and sample standard deviations of the measured parameters described in Materials and Methods for the entire population at various times after mitosis as well as for subpopulations selected by IOD, and Figs. 2, 4, and 5 which display, respectively, the IOD vs. AOD, two parameter histograms, at various times, of the entire population (Fig. 2) and the AOD versus FF histograms for either entire populations or selected (again on the basis of IOD) subpopulations (Figs. 4 and 5).

At 3 h after mitosis, there is little difference between control and treated cells. The ranges of both AOD and FF are the same in the two populations and, although there are slight differences indicative of a more dispersed nuclear morphology in the treated population, it is not completely clear whether these differences are real or rather a statistical fluctuation caused by the sample population size. However, two-tailed statistical tests indicate that the difference in means of the two populations is statistically significant with a significance level of $\leq 2.5\%$.

At 5 h, though, the difference is striking. In examining Table I, we see that a comparison of average values indicates an increase in nuclear condensation accompanied by a change to a more rounded nuclear shape in the theophylline-treated cells. The cause of this difference may be determined by examining the AOD vs. FF histograms. It is clear that the shift in mean values is not caused by the induction by theophylline of a new and abnormal morphological state but rather by the induction

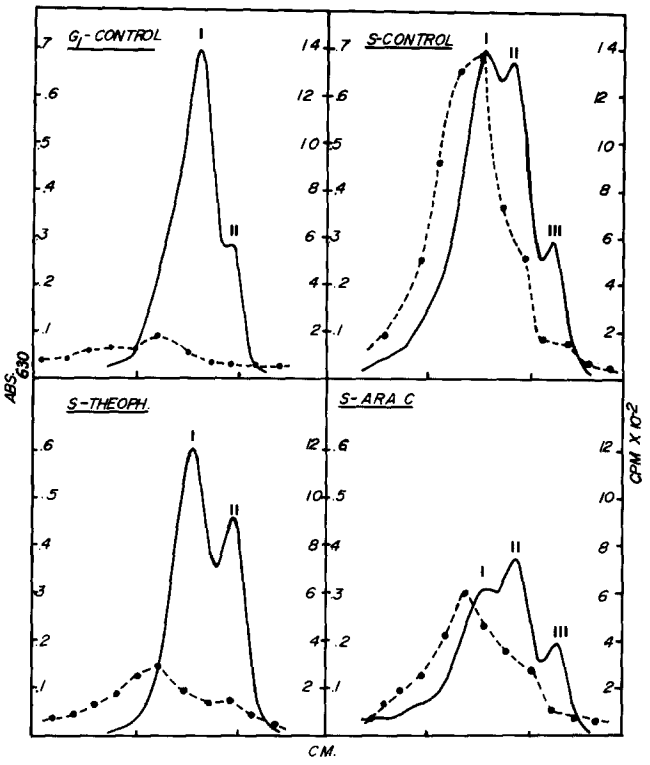

FIGURE 3 The effects of Ara-C and theophylline treatment beginning in G_1 on subsequent histone 1 phosphorylation during the G_1-S transition in HeLa S-3 cells. HeLa cells were collected in mitosis and resuspended in 1,400 ml of medium A at 2.9×10^5 cells/ml and incubated at 37°C. At 2 h after mitosis, 300 ml of cells were harvested and immediately pulse-labeled with ^{32}P (*G_1-CONTROL*). At the same time, 350 ml of cells were treated with Ara-C (40 μg/ml), 350 ml were treated with 5 mM theophylline, and the remaining culture was used as the control. After incubation until 9.5 h mitosis, 300 ml of the control (*S-CONTROL*), Ara-C (*S-ARA C*) and theophylline (*S-THEOPH*)-treated cultures were harvested and pulse-labeled with ^{32}P. For each of the pulses, 8.7×10^7 cells were resuspended in 100 ml of medium A minus phosphate containing 50 μCi/ml [^{32}P]orthophosphate plus 2% fetal calf serum and incubated for 75 min. Histones were isolated and samples derived from the same number of cells were resolved by electrophoresis as described in Materials and Methods. The gels were then stained, scanned at 630 nm, and the radioactivity in 1-mm gel slices was determined as previously described (9). In this figure, the direction of migration (towards the cathode) is on the right and only the regions of the gels containing histone 1 components are shown. The numerals I, II, and III correspond to the three principal peaks containing various histone 1 components which are resolvable under these analytical conditions.—Absorbance at 630 nm; ●, cpm ^{32}P in 1-mm gel slices.

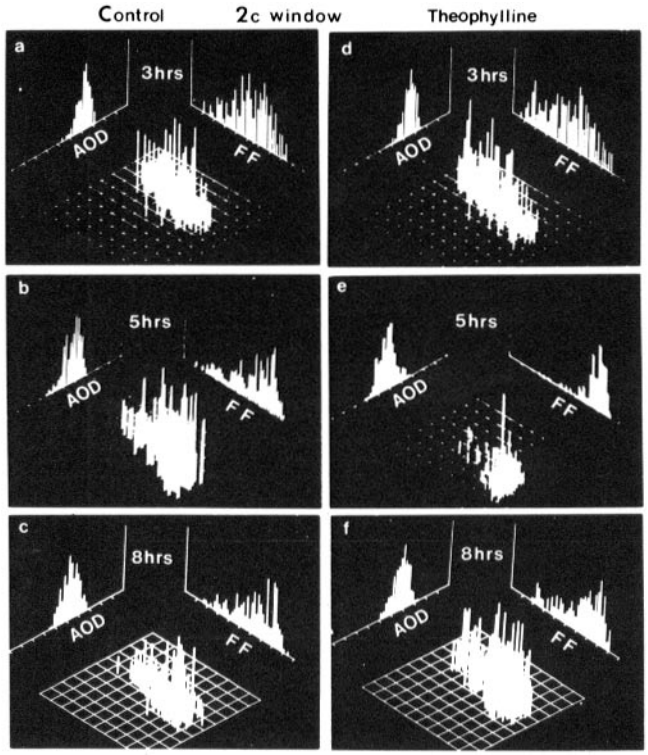

FIGURE 4 AOD and FF histograms for the 2c DNA content subpopulations at 3, 5, and 8 h after selective detachment. The Z axis corresponds to cell number. Each sample population represents between 130 and 200 cells. Histograms *a*, *b*, and *c* correspond, respectively, to the control 2C populations at 3, 5, and 8 h after selective detachment; *d*, *e*, and *f* are corresponding histograms for the theophylline-treated cells. Note particularly the striking difference at 5 h (*b* and *e*).

by theophylline of a marked homogeneity in morphometry. Indeed, 75% of the entire treated population at 5 h falls inside a window of high (40–100 absorbance/unit area) AOD and high FF (0.7–1.0) in which only 30% of the control population is located. It is this same window, which on the basis of previous work (7), has been identified in untreated HeLa cells as characteristic of late G_1.

At 8 h after mitosis, we see that the homogeneity introduced in the theophylline-treated population at 5 h is gone. The distribution of nuclear morphology again resembles that found in the control where the difference, if any, is a slightly increased number of cells with lower AOD in the treated population. Here, two-tailed statistical comparisons of the means for the 2c DNA content subpopulation show significant differences (at a significance level of ~2%) for the AOD and the area, but not for the FF. As noted earlier, in contrast to the apparent similarity in morphometry at this time there is a marked functional difference emerging: roughly 20% of the control populations has entered S phase by this time, as compared to nearly 0% of the treated population.

At 12 h after mitosis, significant morphometrical differences between the two populations re-emerge. In the control population at this time the majority of the cells with DNA content of 2c DNA can be assumed to be in early S phase, based on autoradiography results (5). As shown in Fig. 5, by this time their nuclear morphometry lies in a relatively homogeneous window of low AOD and low FF. Although the theophylline-treated cells also show evidence of the same chromatin relaxation, based on the global averages for AOD and FF found in Table I, this can be seen to be an artifact caused by the different cell cycle phase composition of the two populations. Focusing only on the 2c DNA subpopulations, Table I and Fig. 5 show that there is a significantly higher average AOD and average FF for the treated 2c DNA population as a result of only a fraction of the treated 2c DNA population's having relaxed and altered shape to the extent of the control 2c DNA cells at this time. The remainder of the 2c DNA theophylline-treated cell nuclei, while having experienced a reduction in AOD such that their AOD lies between that of the highly condensed nuclei found in late G_1 and the dispersed nuclei of early S phase, still have maintained the high FF of late G_1 cells. This general distribution pattern is maintained in the 2c DNA-

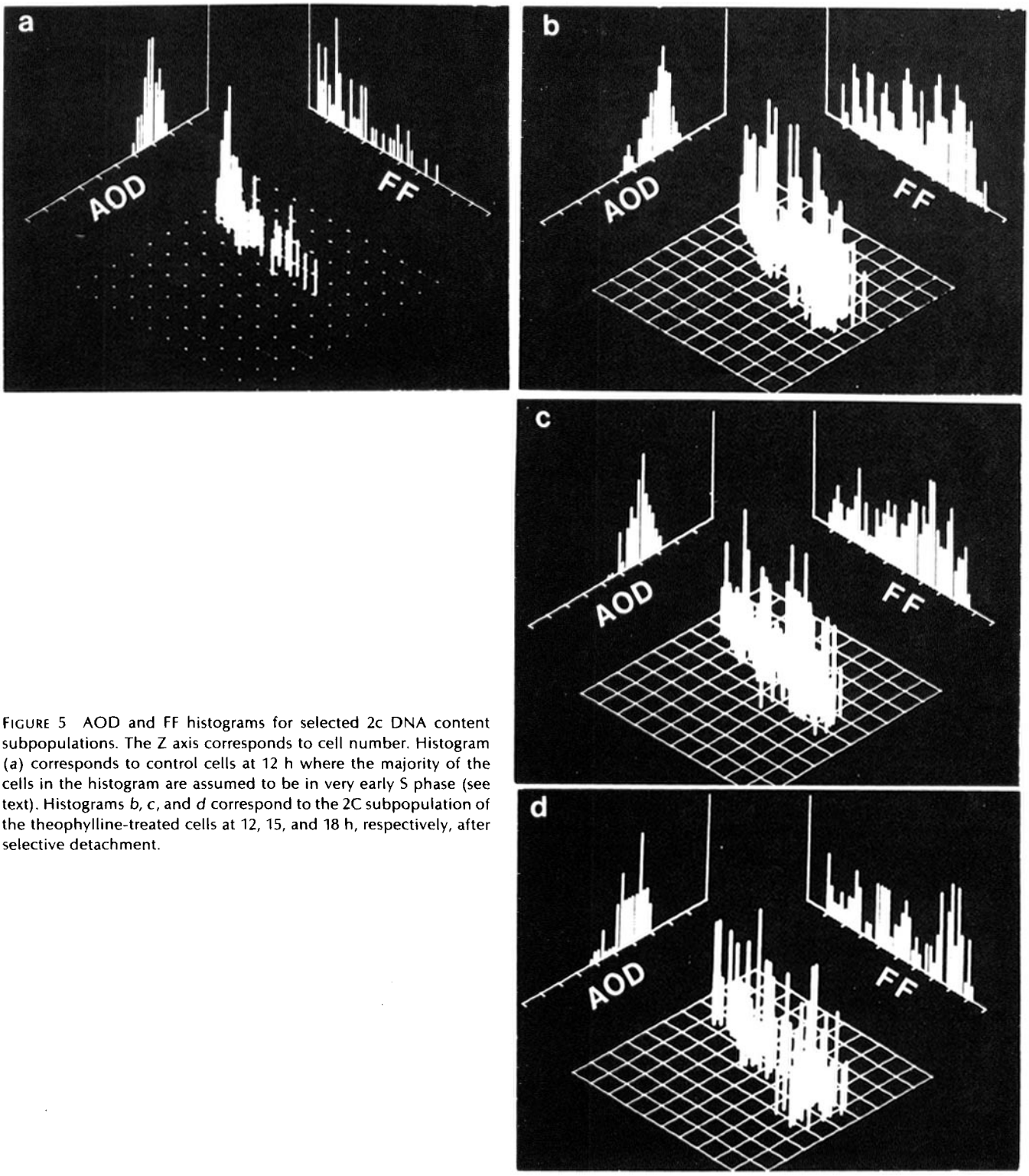

FIGURE 5 AOD and FF histograms for selected 2c DNA content subpopulations. The Z axis corresponds to cell number. Histogram (*a*) corresponds to control cells at 12 h where the majority of the cells in the histogram are assumed to be in very early S phase (see text). Histograms *b*, *c*, and *d* correspond to the 2C subpopulation of the theophylline-treated cells at 12, 15, and 18 h, respectively, after selective detachment.

treated subpopulations at later times (15 and 18 h) as well. Thus, the failure of a large proportion of theophylline-treated cells to enter S phase at the normal time is associated with a failure of their nuclear morphometry to change to the less round forms characteristic of control early S phase and to a lesser extent with the failure of their unclear density to disperse to the extent of control early S phase nuclei.

Finally, examination of Fig. 6 reveals that the modulations in nuclear morphometry decribed above are not related directly to cyclic AMP levels. In agreement with earlier findings (42–44), measurements on the control HeLa cells showed a small increase in cyclic AMP levels between G_1 and S phases. Cellular cyclic AMP levels are lowest at mitosis and increase in an oscillatory manner about twofold during the course of G_1 with a reproducible 10–12% increase at the onset of DNA synthesis (~5 h), decondensation of G_1 chromatin and phosphorylation of H1 (5). Exposure of cells to theophylline produced increases in the cyclic AMP levels to values greater than twice the control

TABLE I

Tabulated Data of Nuclear Morphometry and DNA Content

		IOD	AOD	FF	CF	Area	Perimeter
HeLa theophylline-treated							
3 h	Total	1,908 ± 591	34.2 ± 5.9	0.483 ± 0.211		56.2 ± 15.0	43.0 ± 18.6
5 h	Total	1,727 ± 389	52.0 ± 8.2	0.763 ± 0.109		33.9 ± 8.7	23.8 ± 4.8
8 h	Total						
	2c window (185/198)	1,917 ± 313	41.0 ± 6.6	0.63 ± 19	0.185 ± 0.135	48.1 ± 11.3	32.6 ± 9.7
12 h	Total	1,881 ± 320	36.6 ± 7.3	0.52 ± 0.21	0.265 ± 0.172	53.0 ± 11.2	40.8 ± 18.9
	2c window (166/200)	1,765 ± 95	36.0 ± 7.1	0.51 ± 0.22	0.268 ± 0.175	50.9 ± 9.9	40.4 ± 18.7
	2c-3c window (30/200)	2,309 ± 244	38.3 ± 6.1	0.53 ± 0.19	0.254 ± 0.156	63.0 ± 11.0	43.2 ± 20.3
15 h	Total	2,134 ± 445	39.4 ± 6.8	0.51 ± 0.22	0.272 ± 0.177	55.2 ± 11.9	42.4 ± 19.7
	2c window (128/200)	1,879 ± 67.6	38.4 ± 5.9	0.51 ± 0.21	0.267 ± 0.173	50.2 ± 8.3	40.2 ± 18.4
HeLa untreated							
3 h	Total	1,772 ± 491	37.2 ± 6.2	0.527 ± 0.17		47.9 ± 11	36.1 ± 12
5 h	Total	1,707 ± 329	42.1 ± 7.8	0.62 ± 0.19		41.7 ± 9.6	37.0 ± 10.5
8 h	Total	2,058 ± 388	46.3 ± 7.5	0.63 ± 0.18	0.189 ± 0.122	45.3 ± 8.9	31.4 ± 8.1
	2c window (131/200)	1,880 ± 72	45.3 ± 6.8	0.62 ± 0.18		42.5 ± 7.3	30.9 ± 8.5
12 h	Total	2,761 ± 723	36.5 ± 0.77	0.37 ± 0.22	0.393 ± 0.197	76.5 ± 18.0	64.2 ± 36.8
	2c window (47/200)	1,745 ± 119	29.3 ± 4.3	0.24 ± 0.18	0..519 ± 0.181	60.5 ± 8.1	76.5 ± 43.5
	2c-3c window (58/200)	2,511 ± 321	35.7 ± 5.8	0.35 ± 0.17	0.394 ± 0.163	72.0 ± 12.1	60.0 ± 37.8

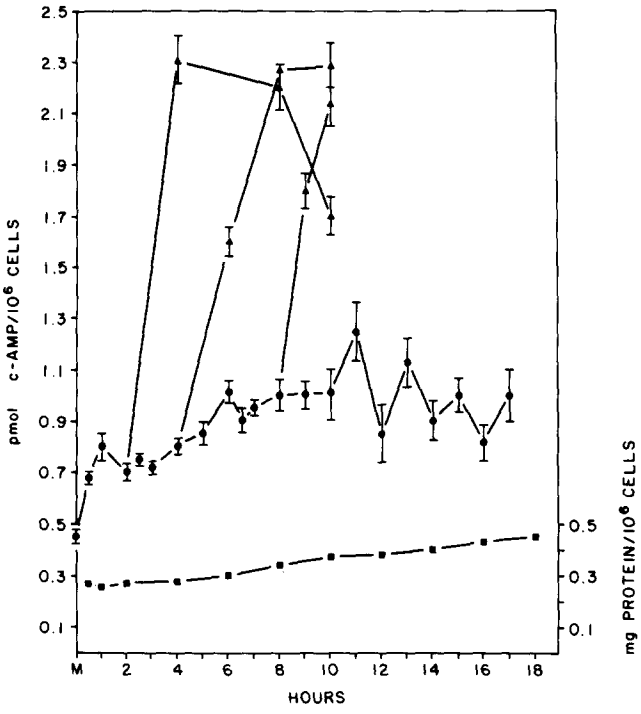

FIGURE 6 Levels of intracellular cyclic AMP during the HeLa cell cycle. Cells were synchronized and cyclic AMP determined as described in Materials and Methods. Theophylline was added to parallel cultures in three independent experiments at 5 mM at 2, 4, and 8 h postmitosis and cyclic AMP was determined. Total cellular protein/10^6 cells was also determined and plotted for data conversion to cyclic AMP/mg protein. Data expressed as panel cyclic AMP/10^6 cells ± 2 SD. ●, Control cells; ▲, 5 mM theophylline; ■, mg protein/10^6 cells.

maximum which peaked depending on the time of administration of the drug between 2 and 4 h after treatment. Although it is interesting to note that the dramatic effect produced by theophylline on nuclear morphology at 5 h after mitosis is coincident with a significant rise in cyclic AMP levels, it must also be noted that even at 10 h the cyclic AMP level in the treated cells is well above the maximum level reached in the control. Moreover, theophylline treatment at 8 h produced similar rises in cyclic AMP but did not affect [^{14}C]thymidine incorporation. Although theophylline causes a 20% rise in cyclic AMP levels 2–4 h after treatment, whether the mid-G_1, late G_1, or early S, this increase did not produce the onset of DNA synthesis or the decondensation of chromatin. Moreover, if theophylline is added in mid-G_1 (2 h), cyclic AMP elevations correlate with condensing of the chromatin into the late G_1 form observed just before the transition to the more extended form observed in early S phase by nuclear morphometry.

DISCUSSION

An analysis of the role of theophylline in producing a delay in the onset and a reduction in the rate of DNA synthesis in synchronized HeLa cells must begin with the observation that the action of theophylline is unrelated to direct interference with the enzymatic apparatus of DNA synthesis as noted earlier in the paper. Rather, its action must be correlated with a critical event(s) occurring normally somewhere between middle and late G_1. Candidates for this event in a simplified approach can be considered roughly to fall into two general categories.

The first possibility is that although theophylline does not act directly on the biochemical pathways of DNA synthesis, it does involve an event in the normal preparation and assembly of the enzymatic apparatus and/or chemical environment required for initiation of DNA synthesis, but that, once initiated, synthesis may continue unaffected by theophylline (Fig. 1). This event might be anything from a change in a specific nucleotide pool size to a reduction in the level of a critical cofactor, to even blocked transcription of a specific enzyme. Such a conclusion, however, must be questioned. It does not explain the theophylline-induced variations in nuclear morphometry reported in this paper unless the same perturbation in the DNA synthesis enzymatic pathways incidentally also produced these same changes or unless these changes are additional events induced by theophylline and independent of the action involving DNA synthesis. Given that the induced morphological structural changes are opposite to those nor-

mally observed in the transition from $G_1 \rightarrow S$, both explanations would assign such an action of theophylline to the status of a mere coincidence.

The alternative hypothesis is that the critical event involves modification of the chromatin structure which, in turn, permits DNA synthesis under those conditions in which the required substrates and enzymes are present and uninhibited, and that theophylline interferes with this normal modification. The observed variations in nuclear morphometry induced by theophylline would now be explained as an expected reflection of interference with this modification. With this hypothesis, interest in the normal association of S phase with histone 1 phosphorylation and the possibility that there exists a causal relationship between histone 1 phosphorylation and chromatin structure is greatly enhanced (5) by the observed inhibition of histone 1 phosphorylation occurring with theophylline treatment.

In summary, then, our results show that the theophylline-induced delay and inhibition of DNA synthesis in synchronized HeLa cells is accompanied by both an arrest of nuclear morphometry in a morphological state intermediate to that of late G_1 and early S and an inhibition of histone 1 phosphorylation. A comparison of data obtained by exposing cells to Ara-C, rather than theophylline, indicates that both the above phenomena are not a direct result of inhibition of DNA synthesis. At present, our best explanation of our results is that the associations between the inhibition of DNA synthesis, the altered nuclear morphometry, and the inhibition of histone 1 phosphorylation are related causally.

This work was supported by grants CA-20034, CA-11463, CA-17896, and CA-25875 from the National Cancer Institute, and IN-143 from the American Cancer Society. C. Nicolini would also like to acknowledge support from the Italian National Research Council.

Received for publication 17 October 1980, and in revised form 1 December 1980.

REFERENCES

1. Kendall, F., R. Swenson, T. Borun, R. Rowinski, and C. Nicolini. 1977. Morphometry during the cell cycle. *Science (Wash. D. C.).* 196:1106.
2. Nicolini, C., W. Giaretti, C. Desaire, and F. Kendall. 1977. The G_0-G_1 transition of WI-38 cells. II. Geometric and densitometric texture analysis. *Exp. Cell Res.* 106:119–125.
3. Kendall, F., F. Beltrame, and C. Nicolini. 1975. Nuclear morphometry in normal and SV-40 transformed human diploid fibroblasts, IEEE. *Trans. Biomed. Eng.* 26:172–175.
4. Nicolini, C. 1979. Chromatin structure, from angstrom to micron levels, and its relationship to mammalian cell proliferation. *In* Chromatin Structure and Function. C. Nicolini, editor. Plenum Press, New York. 613–666.
5. Dolby, T. W., K. Ajiro, T. W. Borun, R. S. Gilmour, A. Zweidler, L. Cohen, P. Miller, and C. Nicolini. 1979. Physical properties of DNA and chromatin isolated from G_1- and S-phase HeLa S-3 cells. Effects of histone H1 phosphorylation and stage-specific nonhistone chromosomal proteins on the molar ellipticity of native and reconstituted nucleoproteins during thermal denaturation. *Biochemistry* 18:1333–1344.
6. Nicolini, C., K. Ajiro, T. W. Borun, and R. Baserga. 1975. Chromatin changes during the cell cycle of HeLa cells. *J. Biol. Chem.* 250:3381–3385.
7. Nicolini, C. 1980. Nuclear morphometry, quinternary chromatin structure, and cell growth. *J. Submicrosc. Cytol.* 12:475–505.
8. Beltrame, F., F. Kendall, and C. Nicolini. 1979. New growth parameters of mammalian cells in suspension and on substrate. *In* Modeling and Simulation. G. Vogt and M. Mickle, editors. Instrument Society of America. 87–94.
9. Marks, D., W. K. Paik, and T. W. Borun. 1973. The relationship of histone phosphorylation to deoxyribonucleic acid replication and mitosis during the HeLa cell cycle. *J. Biol. Chem.* 248:5660–5667.
10. Ord, M. G., and L. A. Stocken. 1968. Variations in the phosphate content and thiol/disulphide ratio of histones during the cell cycle. *Biochem. J.* 107:403–410.
11. Buckingham, R. H., and L. A. Stocken. 1970. Histone F1, purification and phosphorus content. *Biochem J.* 117:157–160.
12. Balhorn, R., W. O. Rieke, and R. Chalkley. 1971. Rapid electrophoretic analysis for histone phosphorylation. A reinvestigation of phosphorylation of lysine-rich histone during rat liver regeneration. *Biochemistry.* 10:3952–3959.
13. Balhorn, R., R. Chalkley, and D. Granner. 1972. A positive correlation with cell replication. *Biochemistry.* 11:1094–1098.
14. Balhorn, R., J. Bordwell, L. Sellers, D. Granner, and R. Chalkley. 1972. Histone phosphorylation and DNA synthesis are linked in synchronous cultures of HTC cells. *Biochem. Biophys. Res. Commun.* 46:1326–1333.
15. Sherod, D., G. Johnson, and R. Chalkley. 1970. Phosphorylation of mouse ascites tumor cell lysine-rich histone. *Biochemistry.* 9:4611–4615.
16. Gurley, L. R., R. A. Walters, and R. A. Tobey. 1973. The metabolism of histone fractions. VI. Differences in the phosphorylation of histone fractions during the cell cycle. *Arch. Biochem. Biophys.* 154:212–218.
17. Gurley, L. R., R. A. Walters, and R. A. Tobey. 1973. Histone phosphorylation in late interphase and mitosis. *Biochem. Biophys. Res. Commun.* 50:744–749.
18. Gurley, L. R., R. A. Walters, and R. A. Tobey. 1974. The metabolism of histone fractions. Phosphorylation and synthesis of histones in late G_1 arrest. *Arch. Biochem. Biophys.* 164: 469–477.
19. Rattle, H. W. E., G. G. Kneale, J. P. Baldwin, H. R. Matthews, C. Crane-Robinson, P. A. Cary, B. G. Carpenter, P. Suau, and E. M. Bradbury. 1979. Histone complexes, nucleosomes, chromatin and cell-cycle dependent modification of histones. *In* Chromatin Structure and Function. C. Nicolini, editor. Plenum Press, New York. 451–513.
20. Matthews, H. R., and E. M. Bradbury. 1978. The role of H1 histone phosphorylation in the cell cycle-turbidity studies of H1-DNA interaction. *Exp. Cell Res.* 111:343.
21. Pastan, I., W. B. Anderson, R. A. Carchman, M. C. Willingham, T. R. Russell, and G. S. Johnson. 1974. Cyclic AMP and malignant transformation. *In* Control of Proliferation in Mammalian Cells. B. Clarkson and R. Baserga, editors. Cold Spring Harbor Laboratory, Cold Spring Harbor, New York. 563–570.
22. Bannai, S., and J. S. Sheppard. 1974. Cyclic AMP, ATP, and cell contact. *Nature (Lond.).* 250:62–64.
23. Sheppard, J. R. 1972. Difference in the cyclic adenosine 3′, 5′ monophosphate levels in normal and transformed cells. *Nat. New Biol.* 236:14.
24. Pastan, I., M. Willingham, R. Carchman, and W. B. Anderson. 1978. Cyclic AMP metabolism in normal and transformed fibroblasts. *In* The Role of Cyclic Nucleotides in Carcinogenesis. J. Schultz and B. G. Gratzner, editors. Academic Press, Inc., New York. 47–52.
25. Otten, J., J. Bader, G. S. Johnson, and I. Pastan. 1972. A mutation in a Rous sarcoma virus gene that controls adenosine 3′, 5′ monophosphate levels and transformation. *J. Biol. Chem.* 247:1632.
26. Burstin, S. J., H. C. Renger, and C. Basilico. 1974. Cyclic AMP levels in temperature-sensitive SV-40-transformed cell lines. *J. Cell Physiol.* 84:69–74.
27. Oey, J., A. Vogel, and R. Pollack. 1974. Intracellular cyclic AMP concentration responds specifically to growth regulation by serum. *Proc. Natl. Acad. Sci. U. S. A.* 71:694.
28. Willingham, M. C., G. S. Johnson, and I. Pastan. 1972. Control of DNA synthesis and mitosis in 3T3 cells by cyclic AMP. *Biochem. Biophys. Res. Commun.* 48:743–748.
29. Sheppard, J. R. 1971. Restoration of contact-inhibited growth to transformed cells by dibutyryl adenosine 3′,5′ cyclic monophosphate. *Proc. Natl. Acad. Sci. U. S. A.* 68:1316–1320.
30. Froehlich, J. E., and M. Rachmeler. 1972. Effect of adenosine 3′,5′ cyclic monophosphate on cell proliferation. *J. Cell Biol.* 55:19–31.
31. Froehlich, J. E., and M. Rachmeler. 1974. Inhibition of cell growth in the G_1 phase by adenosine 3′,5′ cyclic monophosphate. *J. Cell Biol.* 60:249–257.
32. Rozengart, E., and A. B. Pardee. 1972. Opposite effects of dibutyryl adenosine 3′,5′ cyclic monophosphate and serum on growth of Chinese hamster cells. *J. Cell Physiol.* 80:273–280.
33. Chopra, D. 1977. Effects of theophylline and dibutyryl cyclic AMP on proliferation and keratinization of human keratinocytes. *Br. J. Dermatol.* 96:255.
34. Pardee, A., and L. James. 1975. Selective killing of transformed baby hamster kidney (BHK) cells. *Proc. Natl. Acad. Sci. U. S. A.* 72:4994–4998.
35. Walters, R. A., L. R. Gurley, and R. H. Tobey. 1974. Effects of caffeine on radiation-induced phenomena associated with cell-cycle traverse of mammalian cells. *Biophys. J.* 14: 99–118.
36. Terasima, T., and L. J. Tolmach. 1963. Growth and nucleic acid synthesis in synchronously dividing populations of HeLa cells. *Exp. Cell Res.* 30:344–362.
37. Robbins, E., and P. I. Marcus. 1964. Mitotically synchronized mammalian cells: A single method for obtaining large populations. *Science (Wash. D. C.).* 144:1152–1153.
38. Borun, T. W., F. Gabrielli, K. Ajiro, A. Zweidler, and C. Baglioni. 1975. Further evidence of transcriptional and translational control of histone messenger RNA during the HeLa S-3 cycle. *Cell.* 4:59–67.
39. Stein, G. S., and T. W. Borun. 1972. The synthesis of acidic chromosomal proteins during the cell cycle of HeLa S-3 cells. *J. Cell Biol.* 52:292–307.
40. DeCosse, J. J., and N. Aiello. 1966. Feulgen hydrolysis: Effect of acid and temperature. *J. Histochem.* 14:601.
41. Ajiro, K., T. W. Borun., and L. H. Cohen. 1975. Phosphorylation sites of histone 1 (F1) in relation to the cell cycle. *Fed. Proc.* No. 2047 *(Abstr.).*
42. Burger, M. M., B. M. Bombik, B. M. Breckenridge, and J. R. Sheppard. 1972. Growth control and cyclic alterations of cyclic AMP in the cell cycle. *Nat. New Biol.* 239:161–164.
43. Sheppard, J. R., and D. M. Prescott. 1972. Cyclic AMP levels in synchronized mammalian cells. *Exp. Cell Res.* 75:293–296.
44. Millis, A. J. T., G. A. Forrest, and D. A. Pious. 1974. Cyclic AMP dependent regulation of mitosis in human lymphoid cells. *Exp. Cell Res.* 83:335–343.